



## The Impact of Inclined Magnetic Field on Streamlines in a Constricted Lid-Driven Cavity

Merve Gürbüz Çaldağ<sup>1\*</sup>, Ebutalib Çelik<sup>2</sup>

<sup>1\*</sup>TED University, Faculty of Arts and Science, Department of Mathematics, Ankara, Türkiye, [merve.gurbuz@tedu.edu.tr](mailto:merve.gurbuz@tedu.edu.tr)

<sup>2</sup>Çanakkale Onsekiz Mart University, Çanakkale Technical Sciences Vocational School, Department of Computer Technologies, Çanakkale, Türkiye, [e.celik@comu.edu.tr](mailto:e.celik@comu.edu.tr)

\*Corresponding Author

### ARTICLE INFO

### ABSTRACT

Keywords:  
MHD Flow  
Inclination Angle  
Constricted Cavity  
Radial Basis Function (RBF)

The influence of oriented magnetic field on the incompressible and electrically conducting flow is investigated in a square cavity with a moving top wall and a no-slip constricted bottom wall. Radial basis function (RBF) approximation is employed to velocity-stream function-vorticity formulation of MHD equations. Numerical results are shown in terms of streamlines for different values of Hartmann number  $M$ , orientation angle of magnetic field  $\theta$  and the height of the constricted bottom wall  $h_c$  with a fixed Reynolds number. It is obtained that the number of vortices arises as either  $h_c$  or  $M$  increases. However, the increase in  $\theta$  leads to decrease the number of vortices. Formation of vortices depends on not only the strength and the orientation of the magnetic field but also the constriction of the bottom wall.

Article History:  
Received: 15.09.2023  
Accepted: 15.11.2023  
Online Available: 27.02.2024

## 1. Introduction

Flow behaviour in a wavy enclosure has been many industrial applications such as electronic packages, micro-electronic devices, crystal growth, etc. Saidi, Legay-Desesquelles, Prunet-Foch [1] obtained numerical results of the natural convection flow in a sinusoidal cavity by using finite difference method (FDM). They also presented the experimental results of this problem which are good agreement with the numerical ones. Das, Mahmud [2] applied finite volume method (FVM) to solve the Navier-Stokes (N-S) equations coupled with the energy equations. Average Nusselt number and streamlines are depicted for different values of Grashof number and amplitude-wavelength ratios. Layek, Midya [3] studied the impacts of both constriction height and Reynolds number on the incompressible flow in a constricted channel. They implemented the FDM to primitive form of

N-S equations. The influence of wavy top and bottom walls on heat transfer of nanofluids reported in [4]. They showed that including nanoparticle into fluid causes the heat transfer to increase. Mekroussi, Nehari, Bouzit, Chemloul [5] focused on the mixed convection flow in an inclined lid-driven cavity with wavy bottom wall. They indicated that the local Nusselt number attains maximum value at the undulation number is 6 and inclination angle  $120^\circ$ . Natural convection of nanofluids in an inclined cavity with wavy side walls is studied by Ögüt, Akyol, Arıcı [6]. It is found that local Nusselt number decreases with an increase in the inclination angle of the cavity. Azizul, Alsabery, Hashim, Chamkha [7] considered the mixed convection flow in cavity with a wavy bottom wall and moving side walls. Numerical results are depicted for Reynolds, Richardson, Prandtl numbers and the oscillations of the walls by applying finite element method (FEM).

Pirmohammadi, Ghassemi [8] included the magnetic field impact on the heat transfer in a tilted cavity. They solved magnetohydrodynamic (MHD) convection equations for different values of Hartmann and Rayleigh numbers and the inclination angle of the cavity. Öztop, Sakhrieh, Abu-Nada, Al-Salem [9] analyzed the heat transfer of nanofluid in a lid-driven cavity with a hot wavy bottom wall imposed to the horizontal magnetic field. They reported that Hartmann number controls the heat transfer. MHD convection flow in a constricted cavity is studied in [10]. They indicate the contour plots of flow, pressure and temperature for varying the length of the cavity, constriction ratio, Hartmann and Grashof numbers. Khalil, Azzawi, Al-damook [11] performed the MHD free convection in a trapezoidal wavy cavity for various Rayleigh and Hartmann numbers and the number of waves. It is investigated that Rayleigh number increases the heat transfer. Saha, Islam, Yeasmin, Parveen [12] utilized FEM to MHD natural convection flow of nanofluids in an enclosure with wavy top wall exposed to horizontal magnetic field. They obtained that heat transfer is effected by the shape of the nanoparticles.

The impact of magnetic field with an orientation angle on MHD duct flow is analyzed by Aydın, Selvitopi [13]. They implemented the FEM-BEM coupled approach to MHD equations with unbounded external domain. Inclination angle of the magnetic field is considered for MHD mixed convection in parallel plates by Kaladhar, Reddy, Srinivasacharya [14]. Computations carried out for Soret and Hall parameters, Hartmann numbers and inclination angle. They depicted that an increase in the angle decreases the profiles of concentration. Wasif, Mishal, Haque, Haque, Rahman [15] investigated the heat transfer in different cavity shapes subjected to oriented magnetic field.

The effect of the angle of magnetic field on the Nusselt number depends on the aspect ratio of the cavity. Hussain, Öztop [16] focused on the rotation of the magnetic field on power law fluid in a curvilinear cavity with a moving top wall. Influences of various physical parameters on isolines, streamlines and isoconcentration are depicted utilizing FEM. Gürbüz-Çaldağ, Çelik [17] studied the effect of the inclination angle of

magnetic field on Stokes flow in a lid-driven cavity. They showed that the magnitude of the stream function depends on the type of the inclination angle. Selvitopi [18] applied Galerkin FEM to MHD duct flow equations. Impact of the time-varied oblique magnetic field on flow is analyzed. In [19] flow behaviour in a T-Junction is considered under the effect of magnetic field with an angle. Numerical results are obtained in terms of velocity and induced magnetic field by using the stabilized FEM.

To the best of the authors' knowledge the impact of the oriented magnetic field on the flow in a lid-driven cavity with constricted bottom cavity has not been studied yet. We adopt RBF approximation to MHD equations in terms of velocity, stream function and vorticity. The contour plots of stream function are depicted for various values of Hartmann number, orientation of magnetic field and the constriction height of the cavity with a fixed Reynolds number. It is deduced that the constriction causes the formation of new eddies (vortices) with different directions. On the contrary, the augmentation of inclination angle diminishes the number of vortices.

## 2. Mathematical Formulation

The two-dimensional steady flow of a viscous, incompressible and electrically conducting fluid is considered in a square lid-driven cavity whose bottom wall is constricted using the function  $g_b$  such that

$$g_b(x) = \frac{1}{2}h_c(1 + \cos(2\pi(x - \frac{1}{2}))), 0 \leq x \leq 1 \quad (1)$$

where  $h_c$  is the constriction height shown in Figure 1. The uniform inclined magnetic field is exposed to the cavity. This problem is modelled by MHD equations which are obtained from the Navier-Stokes equations of fluid dynamics and Maxwell's equations of electromagnetics through Ohm's law. The non-dimensional form of MHD equations is obtained from the transformations such as

$$(x, y) \rightarrow (xl, yl), \quad (u, v) \rightarrow (uU, vU), \quad (2)$$

$$p \rightarrow pv\rho U/l. \quad (3)$$

In these transformations  $l, U, \rho$  and  $\nu$  are characteristic length, characteristic velocity, density and kinematic viscosity of the fluid, respectively. The non-dimensional MHD equations [20-21] are

$$\nabla \cdot \mathbf{u} = 0 \quad (4)$$

$$\nabla^2 \mathbf{u} = Re(\mathbf{u} \cdot \nabla) \mathbf{u} + \nabla p - M^2(\mathbf{u} \times \mathbf{H}) \times \mathbf{H} \quad (5)$$

where  $\mathbf{H}$  is the magnetic field. Non-dimensional parameters are the Reynolds number and the Hartmann number given as

$$Re = lU/\nu, \quad M = l\mu H_0 \sqrt{\sigma/\rho\nu}, \quad (6)$$

respectively. In these parameters,  $\mu, H_0$  and  $\sigma$  are magnetic permeability, magnetic field intensity and electric conductivity, respectively.

To eliminate pressure terms in the equation (5) MHD equations can be transformed into the stream function-vorticity formulation by using the definition of stream function

$$u = \psi_y, \quad v = -\psi_x \quad (7)$$

and the vorticity

$$\omega = v_x - u_y. \quad (8)$$

Thus, the steady and two-dimensional MHD flow equations in terms of velocity components, stream function and vorticity are

$$\nabla^2 \psi = -\omega \quad (9)$$

$$\nabla^2 \omega = Re \left( u \frac{\partial \omega}{\partial x} + v \frac{\partial \omega}{\partial y} \right) + M^2 \left( -\frac{\partial u}{\partial y} \sin^2 \theta + \left( \frac{\partial v}{\partial y} - \frac{\partial u}{\partial x} \right) \sin \theta \cos \theta + \frac{\partial v}{\partial x} \cos^2 \theta \right) \quad (10)$$

where  $\theta$  is the inclination angle of the magnetic field.

The boundary conditions are

$$u = 0, \quad v = 0, \quad \psi = 0 \text{ on the left wall}$$

$$(x=0, 0 \leq y < 1), \quad (11)$$

$$u = 0, \quad v = 0, \quad \psi = 0 \text{ on the right wall}$$

$$(x=1, 0 \leq y < 1), \quad (12)$$

$$u = 0, \quad v = 0, \quad \psi = 0 \text{ on the bottom wall}$$

$$(y=g_b(x), 0 \leq x \leq 1), \quad (13)$$

$$u = 1, \quad v = 0, \quad \psi = 0 \text{ on the top wall}$$

$$(y=1, 0 \leq x \leq 1). \quad (14)$$

The unknown vorticity boundary conditions are obtained from the stream function equation by using the discretization matrix  $G$  given in the next section.

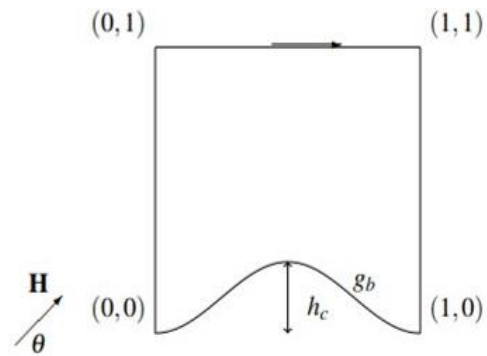


**Figure 1.** Lid-driven cavity with constricted bottom wall.

### 3. Numerical Technique

The radial basis function (RBF) approximation method is employed to solve MHD equations (9)-(10). In RBF technique [22], the inhomogeneity term  $b_1$  of Poisson equation ( $\nabla^2 \tilde{u} = b_1$ ), which is the term except for the Laplacian, is approximated by the RBFs  $\{f_i\}$  as

$$b_1(x, y) = \sum_{i=1}^{NT} \beta_i f_i(r), \quad (x, y) \in \Omega \quad (15)$$

and the approximate solution  $\tilde{u}$  is written

$$\tilde{u}(x, y) = \sum_{i=1}^{NT} \beta_i h_i(r) \quad (16)$$

where  $\{h_i\}$  is obtained from the differential equation

$$\nabla^2 h_i(r) = f_i(r) \quad (17)$$

$$\text{and } r = \sqrt{(x - x_i)^2 + (y - y_i)^2}.$$

The approximate solution  $\tilde{u}$  is forced to satisfy boundary condition

$$B_c \tilde{u} = b_2, \tag{18}$$

we get

$$\sum_{i=1}^{NT} \beta_i B_c h_i(r) = b_2(x, y), (x, y) \in \partial\Omega. \tag{19}$$

Discretizing the boundary  $\partial\Omega$  with  $NB$  points and the domain  $\Omega$  with  $ND$  points gives

$$\sum_{i=1}^{NT} \beta_i B_c h_i(r_j) = b_2(x_j, y_j), 1 \leq j \leq NB \tag{20}$$

$$\sum_{i=1}^{NT} \beta_i f_i(r_k) = b_1(x_k, y_k), 1 + NB \leq k \leq NT = NB + ND. \tag{21}$$

The unknown coefficients  $\{\beta_i\}$  are obtained from the system

$$C\beta = B \tag{22}$$

which is the combination of equation (20) and (21) where

$$C = \begin{bmatrix} B_c h_1(r_1) & B_c h_2(r_1) & \cdots & B_c h_{NT}(r_1) \\ \vdots & \vdots & \ddots & \vdots \\ B_c h_1(r_{NB}) & B_c h_2(r_{NB}) & \cdots & B_c h_{NT}(r_{NB}) \\ f_1(r_{NB+1}) & f_2(r_{NB+1}) & \cdots & f_{NT}(r_{NB+1}) \\ \vdots & \vdots & \ddots & \vdots \\ f_1(r_{NT}) & f_2(r_{NT}) & \cdots & f_{NT}(r_{NT}) \end{bmatrix}_{NT \times NT},$$

$$B = \begin{bmatrix} b_2(x_1, y_1) \\ \vdots \\ b_2(x_{NB}, y_{NB}) \\ b_1(x_{NB+1}, y_{NB+1}) \\ \vdots \\ b_1(x_{NT}, y_{NT}) \end{bmatrix}_{NT \times 1}, \quad \beta = \begin{bmatrix} \beta_1 \\ \vdots \\ \beta_{NT} \end{bmatrix}_{NT \times 1}.$$

The numerical solution

$$\tilde{u} = A[C^{-1}B] \tag{23}$$

is acquired from equation (16) by substituting the coefficients  $\{\beta_i\}$  obtained in the above system (22).

The space derivatives of unknowns are obtained by the discretized matrix

$$G \left( G_{ij} = 1 + r_{ij} \right) \text{ as}$$

$$P_x = G_x G^{-1} P, \quad P_y = G_y G^{-1} P \tag{24}$$

where  $P$  denotes  $u, v, \psi$  and  $\omega$ .

In [23], different RBFs such as quadratic polynomial  $f(r) = 1 + r + r^2$  and multiquadratics  $f(r) = \sqrt{r^2 + c^2}$  with the pre-defined shape parameter  $c$  are used to find solution of MHD Stokes flow in a lid-driven cavity problem. It is deduced that the similar results are obtained, and the linear RBF takes less computational time. In our computation, the iteration takes 210.347s CPU time and 709 iteration step with  $f(r) = 1 + r$  whereas 211.476s time and 710 step with  $f(r) = 1 + r + r^2$  for  $h_c = 0.25, M = 0$  and  $\theta = 0^\circ$ . For that reason, the polynomial RBF  $f(r) = 1 + r$  and the corresponding  $h$  function  $h(r) = \frac{r^2}{4} + \frac{r^3}{9}$  are chosen to find numerical solutions of coupled MHD equations (9)-(10) iteratively.

Iterative procedure is given as:

- Discretized form of the stream function equation (9)

$$\psi^{l+1} = AC^{-1}B \tag{25}$$

is solved by using an initial estimate for the vorticity  $\omega^0$ . The right-hand side matrix  $B$  is obtained by taking

$$b_2(x, y) = 0 \text{ and } b_1(x, y) = -\omega^l. \tag{26}$$

- Velocity components are obtained from the equation (7) with new stream function value such as

$$u^{l+1} = G_y G^{-1} \psi^{l+1}, \quad v^{l+1} = -G_x G^{-1} \psi^{l+1}. \tag{27}$$

- The unknown boundary values of vorticity are obtained from the definition of the vorticity (8)

$$\omega_{bc}^{l+1} = G_x G^{-1} v^{l+1} - G_y G^{-1} u^{l+1}. \tag{28}$$

- We solve the vorticity equation (10)

$$\omega^{l+1} = AC^{-1}B \tag{29}$$

where  $B$  is obtained by taking

$$b_2(x, y) = \omega_{bc}^{l+1} \quad (30)$$

And

$$\begin{aligned} b_1(x, y) = & Re(u_d^{l+1}G_xG^{-1} + v_d^{l+1}G_yG^{-1})\omega^l \\ & - M^2 \sin^2 \theta G_y G^{-1} u^{l+1} \\ & + M^2 \sin \theta \cos \theta (G_y G^{-1} v^{l+1} - \\ & - G_x G^{-1} u^{l+1}) \\ & + M^2 \cos^2 \theta G_x G^{-1} v^{l+1} \end{aligned} \quad (31)$$

$u_d$  and  $v_d$  are diagonal matrices of  $u$  and  $v$  respectively.

- The iteration continues until the preassigned tolerance ( $\xi$ ) is reached between two successive iterations such that

$$\frac{\|\psi^{l+1} - \psi^l\|_\infty}{\|\psi^{l+1}\|_\infty} < \xi, \quad \frac{\|\omega^{l+1} - \omega^l\|_\infty}{\|\omega^{l+1}\|_\infty} < \xi \quad (32)$$

where  $\xi$  is taken  $10^{-6}$  and  $l$  is iteration level.

This iteration is coded with Matlab version R20022a and results are visualized with Tecplot 360EX.

#### 4. Numerical Results

The present iterative RBF approximation is adapted to the steady MHD equations (9)-(10) for various values of Hartmann number ( $0 \leq M \leq 50$ ), inclination angle of the magnetic field ( $0^\circ \leq \theta \leq 90^\circ$ ) and the constriction height  $h_c = 0.25, 0.5$  to analyze the effects of the strength, direction of the magnetic field and the constriction of the cavity on the flow, respectively. Boundary of the cavity is discretized by taking  $NB = 160$  points.  $x$  and  $y$  coordinates of the points [4] are obtained by

$$x_{i+1} = x_i + \Delta x \text{ and } y_{i+1} = y_i + \Delta y \quad (33)$$

where

$$\Delta x = \frac{1}{NB/4} \text{ and } \Delta y = \frac{1-g_b(x)}{NB/4}. \quad (34)$$

The discretization of the domain is depicted in Figure 2. The numerical results are presented in terms of counter plots of stream function in Figures 3-8.

We validate our proposed technique by taking  $M = 0, h_c = 0, Re = 100$ . In this case, our governing equations convert to Navier-Stokes equations in a non-constricted lid-driven cavity so we can compare our results with the solutions obtained by Ghia, Ghia, Shin [24]. In Figures 3-4, it is seen that both the streamlines and the velocity profiles are in well agreement with the results in [24].

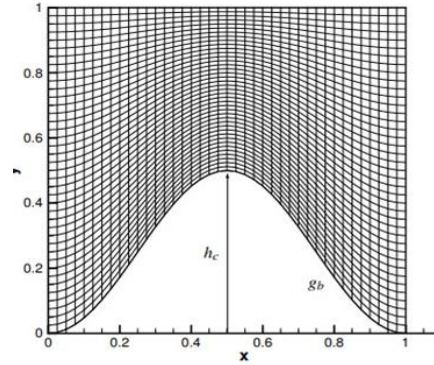


Figure 2. Discretization of the cavity.

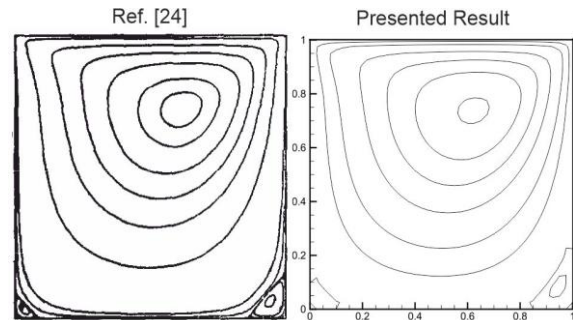


Figure 3. Validation case for  $M = 0$ .

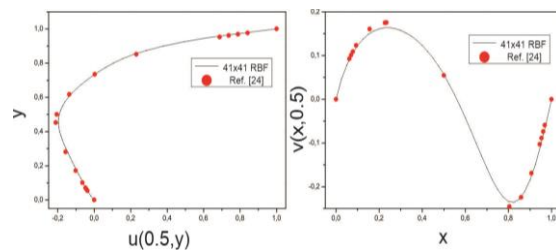
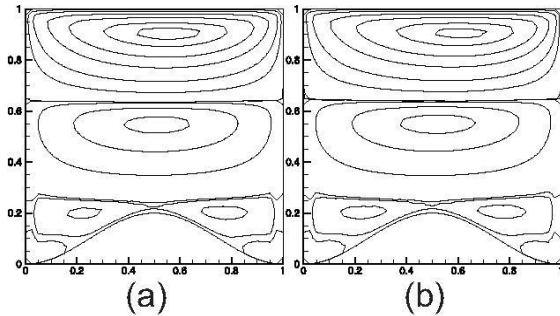


Figure 4. Centerline velocities for  $M = 0$  and  $Re = 100$ .

Also, streamlines are plotted for  $h_c = 0.2, M = 50$  with  $Re = 100$  and  $Re = 200$  as shown in Figure 5. It can be observed that flow patterns are the same. The difference between them is that the position of main vortex as in the Navier-Stokes equations for a single lid driven cavity. More information also can be found in [25].

Besides, our aim is to investigate impact of strength of inclined magnetic field on the streamlines in the cavity with wavy bottom. Thus, we fixed Reynolds number at 100 in our calculations.



**Figure 5.** Flow patterns for  $h_c = 0.2, M = 50$  with (a)  $Re = 100$ , (b)  $Re = 200$ .

After the validation, computations are carried out for different values of  $h_c$  in the absence of magnetic field ( $M = 0$ ) to investigate the impact of constriction on the stream function profiles in Figure 6. For small values of  $h_c$  main vortex of the fluid is located near the top wall due the effect of moving lid and secondary vortices with an opposite direction are formed at the left and right of the constricted area. As  $h_c$  increases to 0.5, the main vortex of the flow shifts through the right part of the cavity. On the other hand, secondary vortices move upward and the formation of new vortex with small value is seen at the left bottom corner.

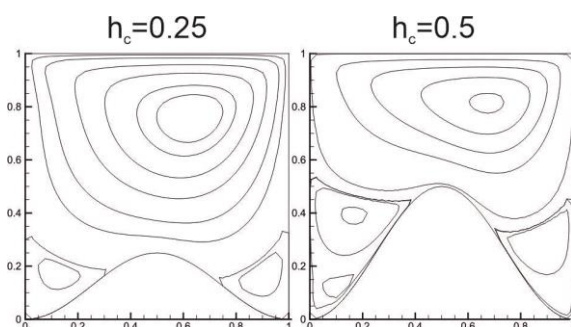


**Figure 6.** Effect of the constriction of the cavity on streamlines for a fixed  $M = 0$ .

Figure 7 demonstrates the effects of both strength and the direction of the magnetic field on the streamline profiles for fixed  $h_c = 0.25$ . When  $\theta = 0^\circ$  which means that magnetic field is applied in the  $x$  –direction, secondary vortices occur at the left and right corners due to the constriction. As Hartmann number increases, the

secondary vortices in the corners move up and bifurcate into main vortex with each other under the first one. The third vortices circulating opposite direction are formed at the bottom corners.

When the inclination angle of the magnetic field is included, flow behaviour is changed. For  $\theta = 45^\circ$  the symmetry of the flow is deformed. The right secondary vortex is larger than the left one due to the direction of the magnetic field. As  $M$  increases, new vortices develop at the right corner. On the contrary, the vorticity at the left corner vanishes. As  $\theta$  reaches to  $90^\circ$ , flow attains symmetric behaviour. For small Hartmann number secondary vortices occur at the bottom corners due the constriction. However, these vortices diminish with an increase in the strength of the magnetic field. Fluid flows in all part of the cavity showing the impact of the moving lid. The augmented in  $M$  causes to form a boundary layer regardless of the direction of the magnetic field.

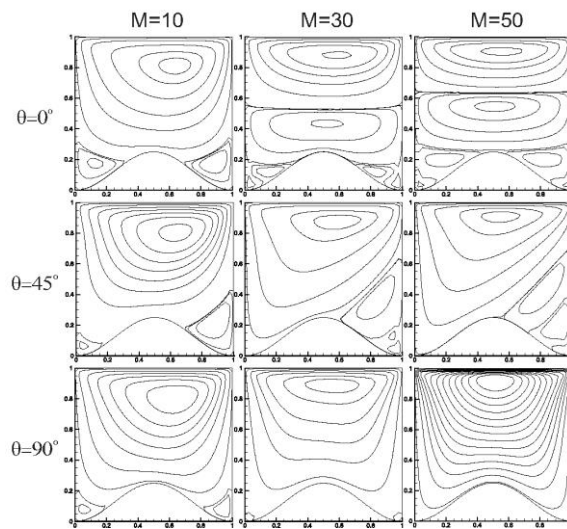


**Figure 7.** Streamlines for a fixed  $h_c = 0.25$ .

In Figure 8 the influences of both  $M$  and  $\theta$  on streamlines are analyzed for different values of  $h_c = 0.25, 0.5$ . In the case of  $\theta = 0^\circ$ , for  $M = 10$  the effect of  $h_c$  on the main vortex and the other vortices are the same as in the case of  $M = 0$  (Figure 6) which shows that the electromagnetic effect on the flow is small. Flow behaviours obtained for fixed  $M = 50$  show that increase in  $h_c$  retards the main effect of Hartmann number on the single secondary vortex formation. It is deduced that the higher constriction ratio requires the higher Hartmann number to form a single secondary vortex. When the inclination

angle increases to  $45^\circ$ , for small values of  $M$  flow behaviours are the same as in the case of  $\theta = 0^\circ$ . However, with a further increase in  $M$  vortices at the left corner due to the constriction diminish. Thus, the direction of the magnetic field controls the development of the new vortices due the constriction.

**Table 1.** Maximum value of  $|\psi|$ .

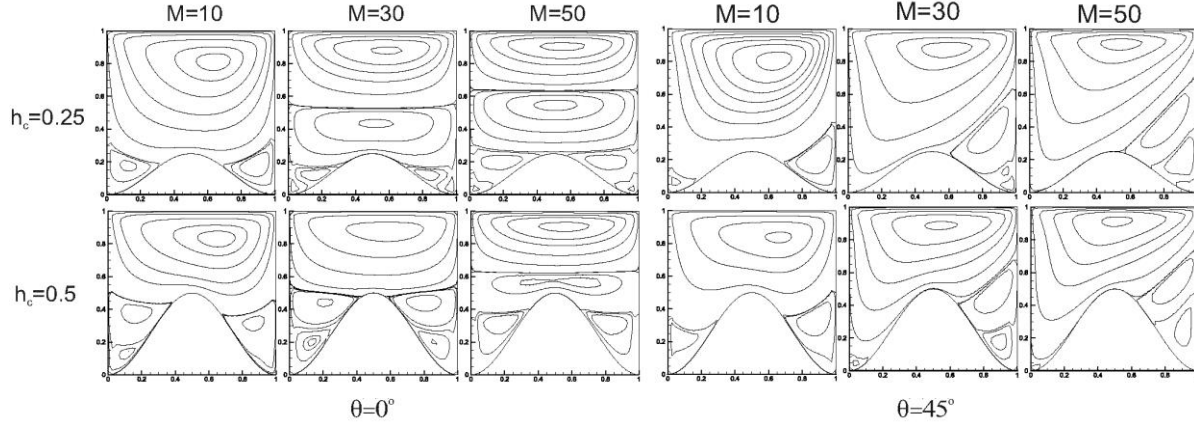
$h_c=0.25$	$M=0$	$M=10$	$M=30$	$M=50$
$\theta = 0^\circ$	0.09369	0.07358	0.04610	0.03568
$\theta = 45^\circ$		0.06817	0.02945	0.01456
$\theta = 90^\circ$		0.06134	0.01980	0.00703
$h_c=0.5$				
$\theta = 0^\circ$	0.07783	0.06899	0.04727	0.03682
$\theta = 45^\circ$		0.06162	0.03061	0.01758
$\theta = 90^\circ$		0.05596	0.02146	0.01045

Table 1 indicates the effects of physical parameters on the maximum value of  $|\psi|$ . In the absence of magnetic field the increase in the constriction decreases  $|\psi|_{max}$ . The same effect is observed for small Hartmann number  $M = 10$ . However, with a further increase in  $M$  as the constriction of the cavity increases, the

maximum value of  $|\psi|$  increases regardless of the direction of the magnetic field. On the other hand, for a fixed  $h_c$ ,  $|\psi|_{max}$  decreases due to the augmentation of  $M$ .

### 5. Conclusion

The behaviour of the flow in a lid-driven cavity with a constricted bottom wall under an applied magnetic field with an inclination angle is analyzed for the first time. The governing MHD equations are solved by using RBF approximation for different values of Hartmann number, inclination angle and the constriction of the cavity. It is deduced that the rotation of the magnetic field plays an important role on the formation of the new vortices due to the constriction. As the inclination angle increases the number of new vortices because of the constriction diminishes. An increase in the Hartmann number decreases the maximum value of  $|\psi|$  regardless of the direction. The flow structure is controlled by the strength of the magnetic field, direction of the magnetic field and the constriction of the cavity.



**Figure 8.** Effects of  $M$  and  $\theta$  on streamlines for  $h_c = 0.25, 0.5$ .

### Article Information Form

#### Funding

The author (s) has no received any financial support for the research, authorship or publication of this study.

#### Authors' Contribution

The authors contributed equally to the study.

#### The Declaration of Conflict of Interest/ Common Interest

No conflict of interest or common interest has been declared by the authors.

#### The Declaration of Ethics Committee Approval

This study does not require ethics committee permission or any special permission.

### ***The Declaration of Research and Publication Ethics***

The authors of the paper declare that they comply with the scientific, ethical and quotation rules of SAUJS in all processes of the paper and that they do not make any falsification on the data collected. In addition, they declare that Sakarya University Journal of Science and its editorial board have no responsibility for any ethical violations that may be encountered, and that this study has not been evaluated in any academic publication environment other than Sakarya University Journal of Science.

### ***Copyright Statement***

Authors own the copyright of their work published in the journal and their work is published under the CC BY-NC 4.0 license.

### **References**

- [1] C. Saidi, F. Legay-Desesquelles, B. Prunet-Foch, "Laminar flow past a sinusoidal cavity", *International Journal of Heat and Mass Transfer*, vol. 30, no. 4, pp. 649–661, 1987.
- [2] P. K. Das, S. Mahmud, "Numerical investigation of natural convection inside a wavy enclosure", *International Journal of Thermal Sciences*, vol. 42, no. 4, pp. 397–406, 2003.
- [3] G. C. Layek, C. Midya, "Effect of constriction height on flow separation in a two-dimensional channel", *Communications in Nonlinear Science and Numerical Simulation*, vol. 12, no. 5, pp. 745–759, 2007.
- [4] E. Abu-Nada, H. F. Oztop, "Numerical analysis of Al<sub>2</sub>O<sub>3</sub>/water nanofluids natural convection in a wavy walled cavity", *Numerical Heat Transfer, Part A: Applications*, vol. 59, no. 5, pp. 403–419, 2011.
- [5] S. Mekroussi, D. Nehari, M. Bouzit, N. E. S. Chemloul, "Analysis of mixed convection in an inclined lid-driven cavity with a wavy wall", *Journal of Mechanical Science and Technology*, vol. 27, pp. 2181–2190, 2013.
- [6] E. B. Ögüt, M. Akyol, M. Arıcı, "Natural convection of nanofluids in an inclined square cavity with side wavy walls", *Isı Bilimi ve Tekniği Dergisi*, vol. 37, no. 2, pp. 139–149, 2017.
- [7] F. M. Azizul, A. I. Alsabery, I. Hashim, A. J. Chamkha, "Heatline visualization of mixed convection inside double lid-driven cavity having heated wavy wall", *Journal of Thermal Analysis and Calorimetry*, vol. 145, pp. 3159–3176, 2021.
- [8] M. Pirmohammadi, M. Ghassemi, "Effect of magnetic field on convection heat transfer inside a tilted square enclosure", *International Communications in Heat and Mass Transfer*, vol. 36, no. 7, pp. 776–780, 2009.
- [9] H. F. Öztop, A. Sakhrieh, E. Abu-Nada, K. Al-Salem, "Mixed convection of MHD flow in nanofluid filled and partially heated wavy walled lid-driven enclosure", *International Communications in Heat and Mass Transfer*, vol. 86, pp. 42–51, 2017.
- [10] M. Tezer, M. Gürbüz, "MHD convection flow in a constricted channel", *Analele Stiintifice Ale Universitatii Ovidius Constanta-Seria Matematica*, vol. 26, no. 2, 2018.
- [11] W. H. Khalil, I. D. Azzawi, A. Al-damook, "The optimisation of MHD free convection inside porous trapezoidal cavity with the wavy bottom wall using response surface method", *International Communications in Heat and Mass Transfer*, vol. 134, p. 106035, 2022.
- [12] T. Saha, T. Islam, S. Yeasmin, N. Parveen, "Thermal influence of heated fin on MHD natural convection flow of nanofluids inside a wavy square cavity", *International Journal of Thermofluids*, vol. 18, p. 100338, 2023.



- [13] S. H. Aydın, H. Selvitopi, “Stabilized FEM-BEM coupled solution of MHD pipe flow in an unbounded conducting medium”, *engineering analysis with boundary Elements*, vol. 87, pp. 122-132, 2018.
- [14] K. Kaladhar, K. M. Reddy, D. Srinivasacharya, “Inclined magnetic field and solet effects on mixed convection flow between vertical parallel plates”, *Journal of Applied Analysis and Computation*, vol. 9, no. 6, pp. 2111–2123, 2019.
- [15] M. Wasif, K. A. Mishal, M. R. Haque, M. M. Haque, F. Rahman, “Investigation of fluid flow and heat transfer for an optimized lid driven cavity shape under the condition of inclined magnetic field”, *Energy and Thermofluids Engineering*, vol. 1, no. 1–2, pp. 47–57, 2021.
- [16] S. Hussain, H. F. Öztop, “Impact of inclined magnetic field and power law fluid on double diffusive mixed convection in lid-driven curvilinear cavity”, *International Communications in Heat and Mass Transfer*, vol. 127, p. 105549, 2021.
- [17] M. Gürbüz-Çaldağ, E. Çelik, “Stokes flow in lid-driven cavity under inclined magnetic field”, *Archives of Mechanics*, vol. 74, no. 6, 2022.
- [18] H. Selvitopi, “Numerical investigation of damped wave type MHD flow with time-varied external magnetic field”, *Chinese Journal of Physics*, vol. 80, pp. 127-147, 2022.
- [19] H. Selvitopi, “Stabilized FEM solution of magnetohydrodynamic flow in different geometries”, *Journal of Scientific Reports-A*, vol. 49, pp. 105-117, 2022.
- [20] H. Yosinobu, T. Kakutani, “Two-dimensional Stokes flow of an electrically conducting fluid in a uniform magnetic field”, *Journal of the Physical Society of Japan*, vol. 14, no. 10, pp. 1433–1444, 1959.
- [21] M. Gürbüz, M. Tezer-Sezgin, “MHD Stokes flow in lid-driven cavity and backward-facing step channel”, *European Journal of Computational Mechanics*, vol. 24, no. 6, pp. 279–301, 2015.
- [22] C. S. Chen, C. M. Fan, P. Wen, “The method of approximate particular solutions for solving certain partial differential equations”, *Numerical Methods for Partial Differential Equations*, vol. 28, no. 2, pp. 506–522, 2012.
- [23] M. Gürbüz, “Radial Basis Function and Dual Reciprocity Boundary Element Solutions of Fluid Dynamics Problems”, Ph.D. dissertation, Department of Mathematics, Middle East Technical University, Ankara, Türkiye, 2017.
- [24] U. Ghia, K. N. Ghia, C. Shin, “High-Resolution solutions for incompressible flow using the Navier-Stokes equations and a multigrid method”, *Journal of Computational Physics*, vol. 48, no. 3, pp. 387–411, 1982.
- [25] E. Çelik, M. Gürbüz-Çaldağ, “Streamline analysis of MHD flow in a double lid-driven cavity”, *Proceedings of the Institution of Mechanical Engineers, Part C: Journal of Mechanical Engineering Science*, vol. 238, pp. 64-74, 2024.